

## Thermoreflectance investigation of zirconium hydrides in the face-centered-tetragonal phase

G. Paolucci\*

*Dipartimento di Fisica, Università degli Studi di Roma I, piazzale Aldo Moro 5, I-00185 Roma, Italy*

E. Colavita

*Dipartimento di Fisica, Università degli Studi Roma I, piazzale Aldo Moro 5, I-00185 Roma, Italy  
and Dipartimento di Fisica, Università della Calabria, I-87036 Arcavacata di Rende,  
Cosenza, Italy and Gruppo Nazionale di Struttura della Materia  
del Consiglio Nazionale delle Ricerche, I-00185 Roma, Italy*

J. H. Weaver

*Department of Chemical Engineering and Materials Science,  
University of Minnesota, Minneapolis, Minnesota 55455*

(Received 2 April 1985)

Thermoreflectance measurements of zirconium hydrides in the face-centered-tetragonal  $\epsilon$ -phase  $ZrH_x$  with  $1.77 \leq x \leq 1.97$  have been performed at room temperature in the 0.7–4.5-eV photon-energy range. Several optical transitions have been singled out and located in the Brillouin zone. They show the  $x$  dependence of interband transitions and permit an experimental band structure for the tetragonal phase.

Zirconium hydrides<sup>1</sup> exhibit a cubic to tetragonal distortion<sup>2,3</sup> for a hydrogen content slightly below the stoichiometric composition  $H/M=2$ . The tetragonal  $\epsilon$  phase of  $ZrH_x$  exists, in fact, as a single and stable phase in the compositional range  $1.74 \leq x \leq 2.0$ .<sup>4</sup> The suggested driving force<sup>5</sup> for the face-centered-cubic (fcc) to face-centered-tetragonal (fct) phase transition<sup>6</sup> is the decrease in the density of states at the Fermi level ( $E_F$ ) with a small shift of  $E_F$  to lower energy. Essentially, the Jahn-Teller effect takes place and an electronic driving force distorts the ideal  $CaF_2$  structure.<sup>2,7</sup>

Band-structure calculations<sup>8</sup> for the fcc phase show a flat, degenerate band running along  $\Lambda$  and crossing  $E_F$  twice, as can be seen in Fig. 1. Accordingly, the Fermi level falls at the center of a very sharp peak in the total density of states,  $N(E)$ .<sup>8</sup> In the  $\epsilon$  phase of zirconium hydride, the total energy is lowered as the band degeneracy is reduced because of the lower crystal symmetry. As a result, two different

bands originate from the  $\Gamma'_{25}-\Lambda-L_3$  band, one below and the other above  $E_F$ . The calculated  $L_3$  splitting for  $TiH_2$  is about 0.2 eV<sup>3</sup> but, experimentally,<sup>9</sup> it appears to be much greater for  $ZrH_2$ .

Thermoreflectance spectroscopy<sup>10</sup> is particularly suitable for studying the electronic properties of metals and alloys. Both critical-point and Fermi-surface transitions can be revealed through line-shape analysis of the derivative spectra.<sup>10-13</sup> The present thermoreflectance investigation allows us to propose an experimental band model for the  $\epsilon$ - $ZrH_x$  system along  $\Lambda$  and  $\Delta$  symmetry lines of the fcc Brillouin zone. This is made possible by spectroscopic trends of the thermoreflectance features as a function of the H content in the  $\epsilon$ - $ZrH_x$  compounds.

The samples used in this study were cut from the same source as those used by Weaver, Peterman, Peterson, and Franciosi in their photoemission<sup>9</sup> and reflectance<sup>14</sup> studies ( $ZrH_x$  with  $x=1.77, 1.87, \text{ and } 1.97$ ). The details of the hydrogen-charging procedure and the sample characterization can be found elsewhere.<sup>9,15</sup> The surfaces were prepared for the present optical measurements by mechanical polishing to a mirror finish. Their size was typically  $2 \times 3 \times 0.1 \text{ mm}^3$ , so that the thermal mass was minimized and the response to temperature modulation was fast. The experiment was conducted at  $T \cong 340 \text{ K}$  because of the base-line increase in temperature while the modulation was in process.<sup>16</sup> The temperature modulation was  $\sim 5 \text{ K}$  and the time constant of the system was compatible with 2 Hz modulation. The data were recorded in the form of temperature-induced changes in reflectance,  $\Delta R/R$ . An accuracy of better than 7% was achieved over the entire spectral energy range, with integration times of 200 sec for each point. In the infrared, particular care was taken to minimize the blackbody contribution. Band-pass optical filters were used and, moreover, the signal was always recorded with and without light.

The details of the experimental technique and the optical layout can be found elsewhere.<sup>16,17</sup> However, the heating system, which has been successfully used in a number of thermoreflectance studies at liquid-nitrogen tempera-

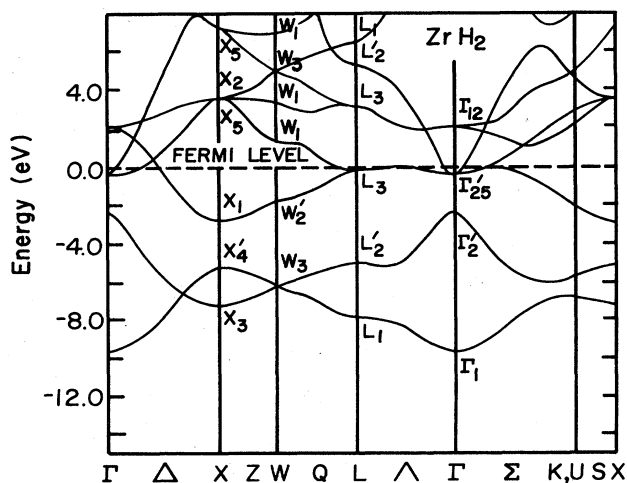


FIG. 1. Energy bands of face-centered-cubic  $ZrH_2$  from Ref. 8.

tures,<sup>12,13,17</sup> was modified to increase its modulation efficiency at room temperature. The old system<sup>17</sup> (a chromium film deposited on a sapphire substrate) could not be used because a pulsed power wave with about 170 W peak-to-peak was dissipated into the heater. Instead, we used a slab of metal-doped graphite ( $0.20 \times 5 \times 35 \text{ mm}^3$ ) fixed on a copper plate by a ceramic glue and having mechanical electrical contacts.<sup>16</sup>

The  $\Delta R/R$  thermoreflectance spectra are shown in Fig. 2. On going from  $\text{ZrH}_{1.77}$  to  $\text{ZrH}_{1.97}$  they become richer in structure, and the peaks at the extremes of the spectral range exhibit ultraviolet and infrared shifts. In contrast, the central features ( $2 < h\nu < 3 \text{ eV}$ ) remain almost invariant in position and shape for all hydride compositions. The features which move can be correlated to regions of the Brillouin zone which are expected to be changed for the  $\text{fcc} \rightarrow \text{fct}$  transition;<sup>2,3,9</sup> structures which do not shift are related to parts of the zone unaffected by the distortion.

The interpretation of  $\Delta R/R$  data is best made through  $\Delta \tilde{\epsilon} = \Delta \epsilon_1 + i\Delta \epsilon_2$  spectra.<sup>10-13</sup> The variation of the imaginary part of the dielectric function,  $\Delta \epsilon_2$ , is directly related to the

change of absorption induced by the temperature modulation. Furthermore, the correlation of structures in  $\Delta \epsilon_1$  and  $\Delta \epsilon_2$  can help to recognize the region in  $k$  space where optical transitions occur. Accordingly, we have determined  $\Delta \epsilon_1$  and  $\Delta \epsilon_2$  spectra through Kramers-Kronig analysis<sup>10</sup> of  $\Delta R/R$ . Outside our spectral energy range,  $\Delta R/R$  was assumed to be structureless, so as to minimize the error introduced by the integration.<sup>18</sup> The static optical constants needed to determine  $\Delta \tilde{\epsilon}$  in the Kramers-Kronig inversion were taken from optical absorptivity measurements<sup>14, 19, 20</sup>

$$\Delta \epsilon_1 = A(\epsilon_1, \epsilon_2) \frac{\Delta R}{R} + B(\epsilon_1, \epsilon_2) \Delta \theta,$$

$$\Delta \epsilon_2 = B(\epsilon_1, \epsilon_2) \frac{\Delta R}{R} + -A(\epsilon_1, \epsilon_2) \Delta \theta.$$

The temperature-induced changes in the dielectric functions of  $\Delta \epsilon_1$  and  $\Delta \epsilon_2$  are shown in Fig. 3. The structures in the low-energy range are the results of two overlapping transitions. Their interpretation as Fermi-surface (FS) transitions<sup>11</sup> is more convincing upon inspection of their line shapes over the range of  $x$  values. The arrows of Fig. 3 indicate the shift to lower energy of the lowest-energy transition as  $x$  increases. For  $\text{ZrH}_{1.77}$ , the two features overlap near 1.5 eV, but they are well separated by  $\text{ZrH}_{1.97}$ . The

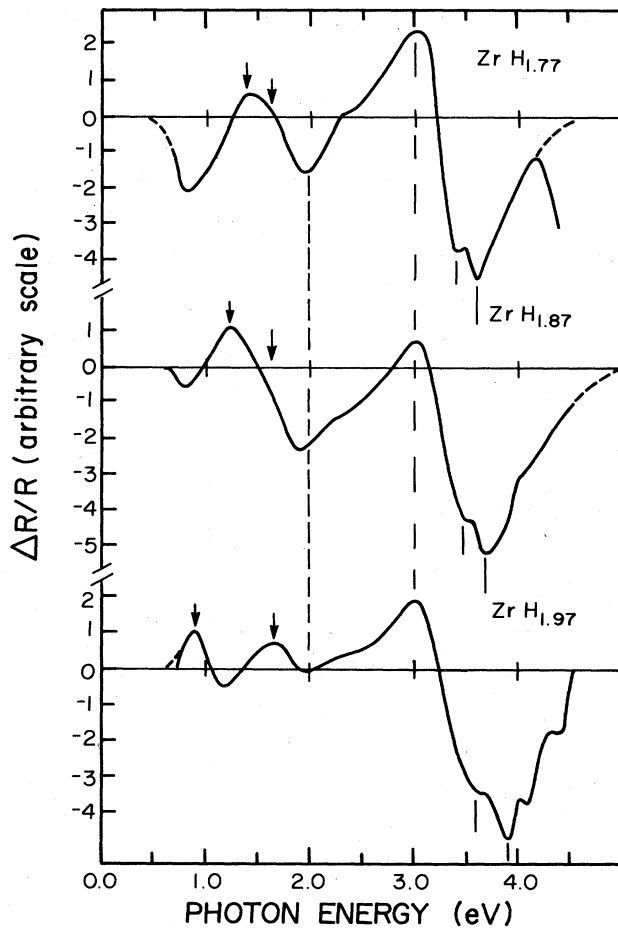


FIG. 2. Thermoreflectance spectra taken at 340 K. The extrapolations used for the Kramers-Kronig analysis are shown as dashed lines. The arrows mark the interband transitions identified in the present work. The structures at higher energy ( $h\nu > 3.5 \text{ eV}$ ) move to the ultraviolet and the low-lying energy features move to the infrared as  $x$  increases.

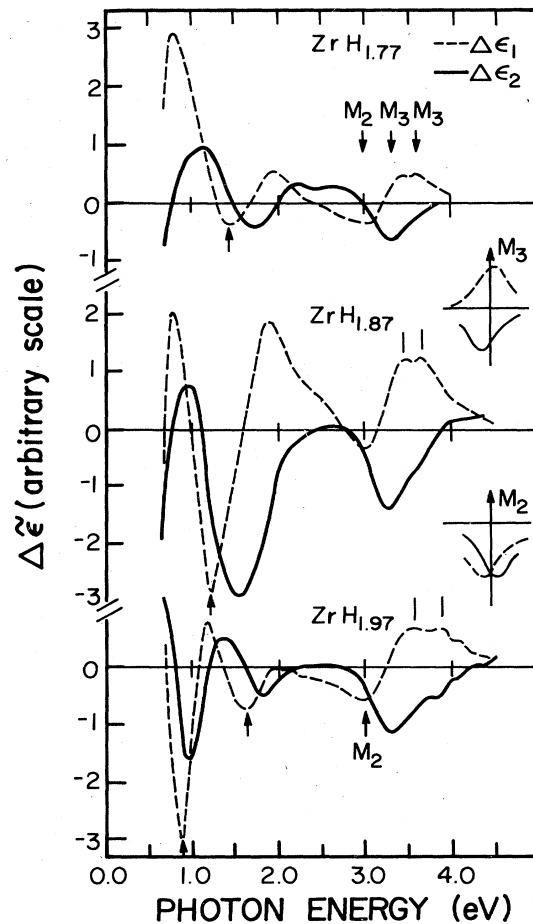


FIG. 3. Temperature variation of the dielectric function. Solid curve is  $\Delta \epsilon_2$ ; dashed curve is  $\Delta \epsilon_1$ . The insets show the theoretical line shapes of  $M_3$  and  $M_2$  critical points (Ref. 10).

corresponding features in  $\Delta R/R$  are more distinct and are consistent with the above interpretation. In fact, starting from the  $ZrH_{1.77}$  spectrum, the two low-lying  $\Delta R/R$  features diverge from  $\sim 1.6$  eV (see pairs of arrows in Fig. 2). Since the  $\Delta R/R$  positive peak of the FS line shape corresponds generally to the onset of this kind of transition,<sup>12,13,21</sup> we can locate the transition easily in  $ZrH_{1.97}$ . For the other two compositions, the precision suffers because of overlap with the second feature<sup>8</sup> (see Table I).

Temperature modulation of the bands of a solid produce well-defined line shapes for bands having particular curvatures in  $k$  space.<sup>10</sup> These critical-point transitions are identified as  $M_2$ -like for bands which curve downward in two  $k$ -space directions and upward in the third (saddle point), and as  $M_3$ -like for bands which curve downward in all three directions (maximum). Temperature modulation of these  $M_2$  and  $M_3$  critical points produces the line shapes shown in the insets of Fig. 3.

In the high-energy range, two  $M_3$  critical points are clearly recognizable in  $\Delta\epsilon$  for each composition. Both move to the ultraviolet on going from  $ZrH_{1.77}$  to  $ZrH_{1.97}$  (as do the  $\Delta R/R$  spectral features), and this suggests their correlation to the increase of the lattice distortion. Once more, we use the structures of  $\Delta R/R$  (negative peaks) to locate the relevant optical transitions.<sup>13,21</sup> This procedure allows us to obtain energy values directly from the experimental results and not from the deconvolution of  $\Delta\epsilon$  structures.

The results of Fig. 3 also show that there is an  $M_2$ -like transition<sup>10</sup> at  $\sim 3$  eV. Another  $M_3$  critical point is recognizable at  $\sim 2$  eV. Both of these remain stationary in energy as  $x$  is varied. We conclude, therefore, that they are related to positions of the Brillouin zone where the fcc  $\rightarrow$  fct distortion has little effect. For the sake of clarity, we note that these two structures (the  $M_2$  and  $M_3$  points) correspond, respectively, to positive and negative peaks in  $\Delta R/R$  spectra.<sup>12,13,21</sup>

The results of this analysis are summarized in Table I. With them, we can propose a qualitative band structure of  $ZrH_x$  in the tetragonal phase, as shown in Fig. 4. Since the Jahn-Teller effect lifts the degeneracy of the doubly degenerate band along  $\Lambda$  in  $ZrH_x$  for  $x \geq 1.77$ ,<sup>2,7,22</sup> we approximate the  $x$ -dependent splitting by rigid shifts of the bands.

The ultraviolet and the infrared shifts of  $\Delta\epsilon$  structures can be correlated to the opening of a gap along  $\Lambda$  and near  $\Gamma$ . More precisely, we assign the two  $M_3$  critical points at  $\sim 3.4$  and  $\sim 3.7$  eV to  $L$  between  $L_3^j$  and  $L_3^k$  (see Fig. 4). Both the shape of initial and final bands and the energy gap make the interpretation quite probable. The infrared shift is even more straightforward to interpret because the two FS

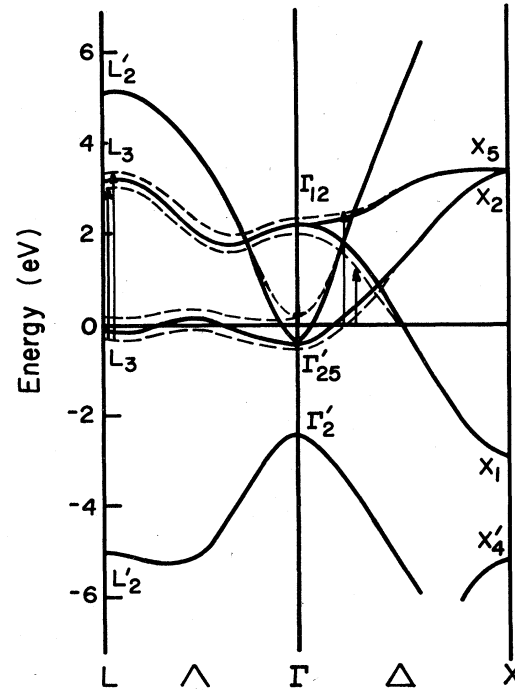


FIG. 4. Proposed band structure of  $\epsilon$ - $ZrH_x$  (dashed lines) and theoretical band structure (Ref. 8) of cubic  $ZrH_2$  (solid lines). The identified interband transitions (see Table I) are consistent with the proposed changes of  $ZrH_2$  band structure due to the tetragonal distortion.

transitions split further apart with  $x$ . Figure 4 provides a qualitative interpretation of their behavior with the lattice distortion. The  $\Delta(E_F) \rightarrow \Delta^4$  transition gets smaller while  $\Delta(E_F) \rightarrow \Delta^5$  is steady or increases slightly as the H content increases (the superscripts denote band index relative to the lowest band). The two bands near  $\Gamma_{12}$  along  $\Delta$  in the fct phase bend differently with increased  $k$ . We can estimate the separation of the final bands ( $\Delta \approx 0.7$  eV in  $ZrH_{1.97}$ ), since the initial state is always at  $E_F$  for both transitions.

Since no other band is expected to cross the Fermi level after the distortion, the above assignment is quite straightforward. However, the  $\Gamma_{12}$  symmetry point needs to be lowered ( $\sim 0.8$  eV) with respect to the theoretical findings<sup>8</sup> unless the distortion gives rise to a more drastic change than we suggest.

Finally, the  $M_2$  critical points at  $\sim 3$  eV and the  $M_3$  critical point at  $\sim 2$  eV can be assigned to  $W$  and  $\Gamma$ , respectively. Transitions at  $W$ , namely,  $W_2' \rightarrow W_1$ , are expected to contribute at  $\sim 3$  eV because the joint density of states (JDOS) is high and dipole rules are satisfied.<sup>8</sup> Indeed, the  $\Delta R/R$  data exhibit a positive peak which does not change with  $x$ , consistent with this assignment. The interpretation of the last  $M_3$  critical point is the least clear. Transitions at  $\Gamma$ , namely,  $\Gamma_{25}' \rightarrow \Gamma_{12}$ , should be allowed in  $ZrH_x$  according to the momentum character decomposition by Gupta.<sup>8</sup> In this case, however, the H-induced shift is not observable and, moreover, the  $M_3$  line shape is unrecognizable in  $ZrH_{1.97}$ . It seems very likely that the presence of nearby absorption makes the recognition difficult. Contributions along  $\Lambda$  and  $\Gamma_2' \rightarrow \Gamma_{25}'$  transitions occur, in fact, at almost

TABLE I. Interband transitions and their proposed location in the Brillouin zone. The energy values are in eV and the uncertainty is 0.05 eV.

Sample	$ZrH_{1.77}$	$ZrH_{1.87}$	$ZrH_{1.97}$	
	$\Delta(E_F) \rightarrow \Delta^3$	1.40	1.25	0.90
	$\Delta(E_F) \rightarrow \Delta^4$	1.60	1.60	1.65
$M_3$	$\Gamma_{25}' \rightarrow \Gamma_{12}$	2.00	2.00	2.00
$M_2$	$W_2' \rightarrow W_1$	3.10	3.10	3.10
$M_3$	$L_3^j \rightarrow L_3^k$	3.30	3.40	3.45
$M_3$	$L_3^j \rightarrow L_3^k$	3.60	3.70	3.90

the same energy, and can modify the original  $M_3$  line shape.

In conclusion, this detailed study of the optical properties of  $ZrH_x$  has made it possible to measure the hydrogen-induced changes in the band structure of the fcc hydride, notably the fcc-fct Jahn-Teller distortion.

We are grateful to Professor R. Rosei for his interest in this research and for helpful discussions. The work at the University of Minnesota was supported by the National Science Foundation under Grant No. DMR-82-16489 of the Solid State Chemistry program.

---

\*Present address: Istituto di Fisica, Università degli Studi di Trieste, via Valerio 2, I-34100 Trieste, Italy.

<sup>1</sup>A. C. Switendick, in *Hydrogen in Metals I: Basic Properties*, edited by G. Alefeld and J. Volkl, Topics in Applied Physics, Vol. 28 (Springer-Verlag, Berlin, 1978).

<sup>2</sup>F. Ducastelle, R. Candron, and P. Costa, *J. Phys. (Paris)* **31**, 57 (1970).

<sup>3</sup>A. C. Switendick, *J. Less-Common Met.* **49**, 283 (1976).

<sup>4</sup>R. L. Beck and W. M. Mueller, in *Metal Hydrides*, edited by W. W. Mueller, J. P. Blackledge, and G. G. Libowitz (Academic, New York, 1968).

<sup>5</sup>M. Gupta, *Solid State Commun.* **29**, 47 (1979).

<sup>6</sup>N. I. Kulikov, F. N. Borzunov, and A. D. Zvonkov, *Phys. Status Solidi B* **86**, 83 (1978).

<sup>7</sup>R. C. Bowman, Jr. and W. K. Rhim, *Phys. Rev. B* **24**, 2232 (1981).

<sup>8</sup>M. Gupta, *Phys. Rev. B* **25**, 1027 (1982).

<sup>9</sup>J. H. Weaver, D. J. Peterman, D. T. Peterson, and A. Franciosi, *Phys. Rev. B* **23**, 1692 (1981).

<sup>10</sup>M. Cardona, *Modulation Spectroscopy*, Solid State Physics, Supplement 11 (Academic, New York, 1969); B. Batz, in *Semiconductors and Semimetals*, edited by R. K. Willardson and A. C. Beer (Academic, New York, 1972), Vol. 9.

<sup>11</sup>R. Rosei, *Phys. Rev. B* **10**, 474 (1974).

<sup>12</sup>E. Colavita, G. Paolucci, and R. Rosei, *Phys. Rev. B* **25**, 7110 (1982).

<sup>13</sup>E. Colavita, A. Franciosi, C. Mariani, and R. Rosei, *Phys. Rev. B* **27**, 4684 (1983).

<sup>14</sup>J. H. Weaver (unpublished). See J. H. Weaver, R. Rosei, and D. T. Peterson, *Phys. Rev. B* **19**, 4855 (1979) for experimental details of the optical calorimeter.

<sup>15</sup>See Weaver, Rosei, and Peterson, Ref. 14.

<sup>16</sup>E. Colavita, G. Paolucci, G. Falasca, and S. Plutino, *J. Phys. D* **17**, 1889 (1984).

<sup>17</sup>E. Colavita, S. Modesti, and R. Rosei, *Phys. Rev. B* **14**, 4315 (1976).

<sup>18</sup>A. Balzarotti, E. Colavita, S. Gentile, and R. Rosei, *Appl. Opt.* **14**, 2412 (1975).

<sup>19</sup>Because of the lack of static optical measurements on an extended energy range, the absorptivity data (Ref. 14) were extrapolated by a Drude-like behavior in the infrared, while the Zr static constants were used for the high-energy range. It has been assumed that the core level absorption of these hydrides would qualitatively resemble those of the metal itself.

<sup>20</sup>D. W. Lynch, C. G. Olson, and J. H. Weaver, *Phys. Rev. B* **11**, 3617 (1975).

<sup>21</sup>The interpretation of  $\Delta R/R$  line shapes is often misleading (see Ref. 13), but the onset of the interband transitions generally corresponds to maxima or minima of  $\Delta R/R$ .

<sup>22</sup>R. C. Bowman, Jr., E. L. Venturini, B. D. Craft, A. Attalo, and D. B. Sullenger, *Phys. Rev. B* **27**, 1474 (1983).